Nano Research 2016, 9(2): 363–371
DOI 10.1007/s12274-015-0915-7
Research Article

ISSN 1998-0124
CN 11-5974/O4

Radio frequency transistors based on ultra-high purity semiconducting carbon nanotubes with superior extrinsic maximum oscillation frequency

Yu Cao[1,§], Yuchi Che[1,§], Hui Gui[2], Xuan Cao[2], and Chongwu Zhou[1,2] (✉)

[1] *Department of Electrical Engineering, University of Southern California, Los Angeles, CA 90089, USA*
[2] *Department of Chemical Engineering and Materials Science, University of Southern California, Los Angeles, CA 90089, USA*
[§] *These authors contributed equally to this work.*

Received: 6 August 2015
Revised: 23 September 2015
Accepted: 5 October 2015

© Tsinghua University Press and Springer-Verlag Berlin Heidelberg 2015

KEYWORDS
carbon nanotube,
ultra-high purity,
radio frequency transistors,
maximum oscillation frequency,
T-shape gate

ABSTRACT

In this paper, we report polyfluorene-separated ultra-high purity semiconducting carbon nanotube radio frequency transistors with a self-aligned T-shape gate structure. Because of the ultra-high semiconducting tube purity and self-aligned T-shape gate structure, these transistors showed an excellent direct current and radio frequency performance. In regard to the direct current characteristics, these transistors showed a transconductance up to 40 μS/μm and an excellent current saturation behavior with an output resistance greater than 200 kΩ·μm. In terms of the radio frequency characteristics, an extrinsic maximum oscillation frequency (f_{max}) of 19 GHz was achieved, which is a record among all kinds of carbon nanotube transistors, and an extrinsic current gain cut-off frequency (f_T) of 22 GHz was achieved, which is the highest among transistors based on carbon nanotube networks. Our results take the radio frequency performance of carbon nanotube transistors to a new level and can further accelerate the application of carbon nanotubes for future radio frequency electronics.

1 Introduction

Carbon nanotubes with their characteristics of small size, high carrier mobility, large current density, and small intrinsic capacitance [1–3] provide great potential for next-generation electronics, including digital electronics, macro-electronics, and analog electronics. For digital electronics, several groups have demonstrated basic logic blocks and complex circuits built from carbon nanotubes, such as inverters, NAND gates, NOR gates, decoders, ring oscillators, and computers [4–8]. In addition, carbon nanotubes are also widely studied for macro-electronics, including flexible electronics and printed electronics [9–16]. Fabricated/printed thin-film carbon nanotube transistors on rigid/flexible substrates have been shown to drive an active-matrix organic light emitting diode (AMOLED) [10, 11] and to control various kinds of sensors [14, 15],

Address correspondence to chongwuz@usc.edu

e.g., light sensors and tactile sensors. Moreover, carbon nanotubes are also considered one of the most promising materials for radio frequency (RF) analog electronics because of their excellent intrinsic properties [3, 17–27]. In order to achieve a good RF performance, carbon nanotubes from different assembling methods with various transistor structures have been explored comprehensively.

In terms of carbon nanotubes assembling methods, aligned carbon nanotubes from the chemical vapor deposition (CVD) process [28–30] can be used without removing metallic nanotubes to make RF transistors, even though carbon nanotubes from CVD process are a mix of both semiconducting and metallic carbon nanotubes. Several research groups including our group have made RF transistors with CVD aligned carbon nanotubes [23, 25, 26]. However, as metallic carbon nanotubes have no gate modulation, the RF performance of aligned carbon nanotube transistors can be harmed due to the existence of metallic carbon nanotubes. Besides the aligned carbon nanotubes obtained from the CVD process, carbon nanotube networks achieved by dispersing pre-separated carbon nanotube solutions [19–21] can also be used to make RF transistors. Although, carbon nanotube networks are used as the channel material, the carrier transport can be quasi-ballistic transport instead of percolative transport because of the small channel length [21]. As a result, the RF performance of carbon nanotube network transistors can be as good as that of aligned carbon nanotube transistors. Researchers including our group have reported good RF performance of carbon nanotube network transistors [19–21]. Other types of carbon nanotubes, such as single carbon nanotubes [17, 22, 27] and nanotubes aligned by dielectrophoresis (DEP) method [18, 24], have also been made into RF transistors and characterized.

The device structure is also of great importance for the RF performance of carbon nanotube transistors. Top/back-gate structure without self-alignment is a commonly used gate structure for these transistors [17–20, 24–26]. The major drawback of this structure is that there exist either un-gated channel regions or overlapped gate-to-source/drain regions. The un-gated channel regions adversely affect the RF performance of transistors because they cannot be controlled by the gate and incur large access resistance. The total length of the un-gated channel regions is determined by the alignment during the manufacturing process. Besides the un-gated channel regions, the overlapped gate-to-source/drain regions also incur large parasitic capacitance, which negatively affects the RF performance of carbon nanotube transistors. A better gate structure is a top-gate structure with self-alignment. Several research groups including our group have reported RF transistors with such a gate structure [21–23, 31, 32]. Our group introduced a self-aligned T-shape gate structure for RF transistors and successfully made RF transistors using this gate structure with dispersed carbon nanotube networks [21], aligned carbon nanotubes [23], and graphene [32]. This self-aligned T-shape gate structure not only reduces the parasitic capacitance, but also decreases the gate resistance and improves the yield of devices as compared with the gate structures without self-alignment.

In spite of the intensive research in carbon nanotube RF field, the RF performance of carbon nanotube transistors is still lower than that of the current state-of-the-art transistors, particularly for the maximum oscillation frequency (f_{max}), which is an important parameter for practical applications. The best extrinsic f_{max} so far reported for carbon nanotube transistors is 15 GHz [24]. In order to achieve better RF performance, particularly a high value of f_{max}, for practical applications, it is critical to achieve both high transconductance and good current saturation for carbon nanotube transistors. The transconductance and current saturation behavior of carbon nanotube transistors are directly related to the purity of the semiconducting carbon nanotube. Metallic carbon nanotubes, which have no gate modulation and conduct current similar to a metal wire, degrade the transconductance and current saturation behavior. As a result, the higher the purity of the semiconducting carbon nanotubes, the higher the transconductance and the better the current saturation behavior can be achieved. Combining the ultra-high purity semiconducting carbon nanotubes and the excellent self-aligned T-shape gate structure, improved RF performance, especially for f_{max}, can be expected.

In this work, polyfluorene-separated ultra-high purity (> 99.99%) semiconducting carbon nanotubes

are used for the radio frequency study. We fabricated the self-aligned T-shape gate transistors and carried out both the direct current (DC) and RF characterizations. Ultra-high purity semiconducting carbon nanotube RF transistors showed a transconductance up to 40 μS/μm and an excellent current saturation behavior with an output resistance greater than 200 kΩ·μm. RF measurements showed an extrinsic f_{max} of 19 GHz, which is a record among all kinds of carbon nanotube transistors. Furthermore, the RF measurement showed an extrinsic current gain cut-off frequency (f_T) of 22 GHz, which is the highest among transistors based on carbon nanotube networks (the best extrinsic f_T previously reported for carbon nanotube network transistors is 15 GHz [19]) and is comparable to the best extrinsic f_T so far reported for aligned carbon nanotube transistors (25 GHz [23]). Moreover, we studied the linearity behavior of ultra-high purity semiconducting carbon nanotube RF transistors. The transistors showed a 1-dB gain compression point (P_{1dB}) between 8 to 14 dBm and an input third-order intercept point (IIP_3) of 18.3 dBm (the associated output third-order intercept point (OIP_3) is 2.2 dBm). At last, we configured the ultra-high purity semiconducting carbon nanotube transistors as mixers working in GHz frequency range. Our study provides a guideline for material selection for carbon nanotube RF electronics. Most significantly, our ultra-high purity semiconducting carbon nanotube transistors create a record extrinsic f_{max}, push the frontier of carbon nanotube RF field ahead, and further confirm the great potential of carbon nanotubes to be used for future RF analog electronics.

2 Results and discussion

Polyfluorene-separated ultra-high purity (> 99.99%) semiconducting carbon nanotube solution purchased from NanoIntegris (IsoSol-S100, S23-189) was used to make RF transistors with self-aligned T-shape gate structure. Figure 1(a) shows the absorption spectrum of the carbon nanotube solution. There is no visible peak in the metallic regime (600 to 800 nm). The carbon nanotube solution was then dispersed onto a quartz substrate to form a uniform and high-density network. The dispersion method, as described in section 4, is highly scalable and enables large-scale fabrication of RF transistors and circuits. Figure 1(b) shows a field emission scanned electron microscope (FESEM) image of a high-density and uniformly-dispersed carbon

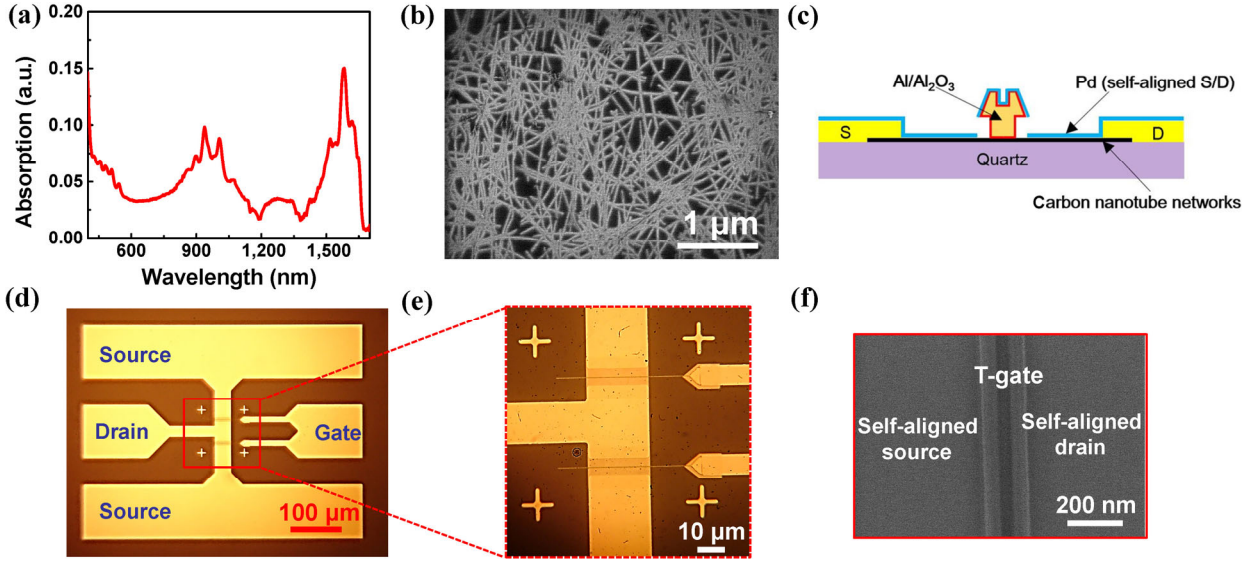

Figure 1 Characterization of ultra-high purity semiconducting carbon nanotubes and self-aligned T-shape gate RF transistors. (a) Absorption spectrum of ultra-high purity semiconducting carbon nanotube solution. (b) Scanning electron microscope image of the ultra-high purity semiconducting carbon nanotube network. (c) Schematic of the self-aligned T-shape gate device structure. (d) Optical image of a typical RF transistor with channel length 2 × 30 μm. (e) Zoomed-in optical image of the channel region in (d). (f) Scanning electron microscope image of the T-shape gate structure.

nanotube network. Using the ultra-high purity semiconducting carbon nanotube network on quartz substrate, we fabricated radio frequency transistors with self-oxidized and self-aligned T-shape aluminum gate platform developed by our group [21, 23, 32]. Figure 1(c) illustrates the schematic of the self-aligned T-gate device structure. The details for carbon nanotube RF transistor fabrication process can be found in section 4. Ground-signal-ground (GSG) coplanar waveguide structure was used to probe the RF performance of the carbon nanotube transistors, as shown in the optical image in Fig. 1(d). Figure 1(e) shows the zoomed-in optical image of the device's channel region. The structure of the RF transistor was further characterized by FESEM. Figure 1(f) illustrates the self-aligned T-shape gate structure. The channel length is estimated to be between 120 to 140 nm and the un-gated region of each side is about 20 nm.

We first carried out DC characterization of the ultra-high purity semiconducting carbon nanotube transistors. Figure 2(a) shows the transfer characteristics (I_{DS}–V_{GS} curve) of one channel of a typical device with a channel width of 30 μm and channel length of 120 nm, with the drain biased at –1.5 V and the source grounded. One can observe that the transfer curve shows a p-type transistor behavior with hysteresis, which is typical for carbon nanotube transistors. The transistor has a high on-state current density (I_{on}/W) of about 37 μA/μm, measured at V_{ds} = –1.5 V and V_{gs} = –1.5 V. The off-state current density (I_{off}/W), measured at V_{ds} = –1.5 V and V_{gs} = 0.6 V, is about 0.7 μA/μm. With both on-state and off-state current density, the on/off ratio is calculated to be 60. Further, the transconductance of the same transistor is calculated by taking derivative of the transfer curve and plotted in Fig. 2(b). A maximum transconductance of 40 μS/μm is achieved at V_{ds} = –1.5 V and V_{gs} = –1.5 V. The peak transconductance is higher than that of 98% purity semiconducting carbon nanotube transistors (~20 μS/μm) [21]. Output characteristics (I_{DS}–V_{DS} curves) are another important aspect of the DC performance of a transistor. Figure 2(c) shows the output characteristics of the same device measured at different gate biases. The drain-to-source voltage was swept from 0 to –2 V and the gate bias was swept from 0 to –1.5 V with a step size of –0.3 V. The device shows better current saturation than the 98% purity semiconducting carbon nanotube transistors [21]. The output resistance of the ultra-high purity semiconducting carbon nanotube transistors is extracted to be larger than 200 kΩ·μm in their current saturation regions, while the output resistance of the 98% purity semiconducting carbon nanotube transistors is only ~60 kΩ·μm. In summary, ultra-high purity semiconducting carbon nanotube transistors have higher transconductance and better current saturation behavior than the previously reported transistors with 98% purity semiconducting carbon nanotube transistors [21]. The higher transconductance and better current saturation behavior is due to the ultra-high purity of the semiconducting carbon nanotubes. Metallic carbon nanotubes show linear output behavior without current saturation with the drain-to-source voltage that we use. As a result, the presence of metallic carbon nanotubes can significantly hurt the current saturation behavior. In addition, metallic carbon nanotubes have no gate dependence and semi-metallic carbon nanotubes have rather small gate modulation. Therefore, the presence of metallic or semi-metallic carbon nanotubes may also degrade the transconductance.

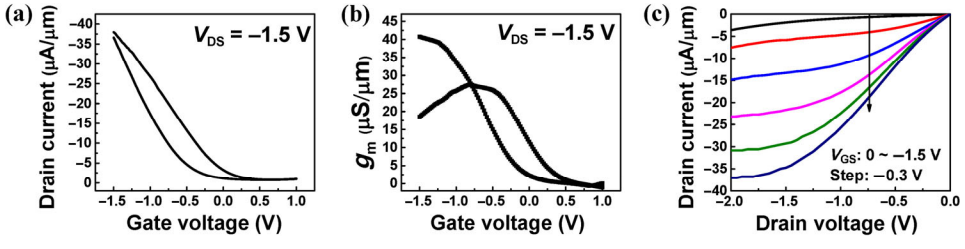

Figure 2 DC characterization of ultra-high purity semiconducting carbon nanotube transistors. (a) Transfer characteristics (I_{DS}–V_{GS} curves) of a nanotube device with a channel width of 30 μm and channel length of 120 nm at the drain-to-source bias of –1.5 V. (b) Transconductance, g_m vs. gate voltage, V_{GS} curve of the same transistor at drain-to-source bias of –1.5 V. (c) Output characteristics (I_{DS}–V_{DS} curves) of the same transistor at various gate biases from 0 to –1.5 V with a step size of –0.3 V.

Two figures of merit are used to characterize the RF performance of a transistor. One is the current gain cut-off frequency and the other is maximum oscillation frequency. The current gain cut-off frequency is the frequency at which the ratio of the output current to the input current equals unity assuming that the output of the transistor is shorted to ground. The maximum oscillation frequency is the frequency at which the ratio of output power to the input power equals unity, assuming that the output is terminated to the characteristic impedance of the system. The maximum oscillation frequency is of more importance than the current gain cut-off frequency since output terminals are usually matched to the characteristic impedance in practical applications. To characterize the RF performance of ultra-high purity semiconducting carbon nanotube RF transistors, standard S-parameter measurement utilizing GSG probes and N5242A PNA-X vector network analyzer was carried out. The N5242A PNA-X network analyzer and the entire measurement setup were first calibrated using standard short-open-load-through (SOLT) calibrations. Moreover, open and short device structures were measured for the de-embedding process, which removes the effects of parallel and series parasitics associated with the measurement pads and connections. The open and short structures for the de-embedding process are shown in Fig. S1 of the Electronic Supplementary Material (ESM). Our de-embedding process only removes the effect of the bonding pads and reveals the real performance of the devices without bonding pads, but with the fringe capacitances between the gate and the source/drain electrodes, which represent the device performance for real applications. We note that some other de-embedding processes used in literature [19, 23, 24] remove the effect of fringe capacitances, which may reveal the upper-limit of the material property, but do not represent the device performance that one can achieve in real circuits. Figures 3(a) and 3(b) plot the extrinsic and intrinsic current gain frequency response and power gain frequency response of the carbon nanotube network devices, respectively. The f_T before and after de-embedding is 22 and 28 GHz, respectively, and the f_{max} before and after de-embedding is 19 and 25 GHz, respectively. Both f_T and f_{max} of the ultra-high purity semiconducting carbon nanotube transistors are better than those of 98% purity semiconducting carbon nanotube transistors with the same device structure [21]. Besides, the extrinsic f_T is the highest for carbon nanotube network transistors (the best extrinsic f_T previously reported for carbon nanotube network transistors is 15 GHz [19]), and it is comparable to the best value so far reported for aligned carbon nanotube transistors (25 GHz [23]). Moreover, the extrinsic f_{max} of ultra-high purity semiconducting carbon nanotube transistors creates a record for all kinds of carbon nanotube RF transistors, and the intrinsic f_{max} is comparable to the best value so far reported. Previously, the best extrinsic and intrinsic f_{max} reported were 15 and 30 GHz, respectively [24]. Again, the improved performance can be attributed to the ultra-high purity of the semiconducting carbon nanotubes, which leads to higher transconductance and better current saturation behavior. In addition, we conducted a statistical study on the RF performance of the ultra-high purity semiconducting carbon nanotube transistors and the results are shown in the ESM (Table S1). From the statistical results, it can be seen that the ultra-high purity semiconducting carbon nanotube transistors show small device-to-device variation.

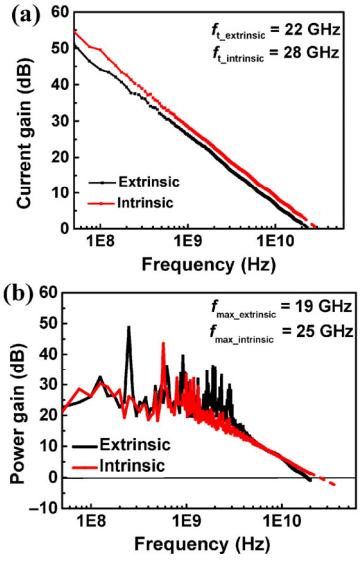

Figure 3 RF characterization of ultra-high purity semiconducting carbon nanotube transistors. (a) Extrinsic and intrinsic current gain frequency response. (b) Extrinsic and intrinsic power gain frequency response.

Another important figure of merit to evaluate an RF transistor is its linearity performance. Two parameters are often used to characterize the linearity of a transistor, circuit or system. One parameter is the 1 dB gain compression point, which defines the power level that causes the gain to drop by 1 dB from its small signal value. The other one is the third-order intercept point where the power of the third-order harmonic term equals the power of the fundamental term. Single-tone test and two-tone test are often used to get the 1 dB gain compression point and the third-order intercept point, respectively. Figure 4(a) shows the schematic of the measurement setup for the single-tone and two-tone tests. For the single tone test, only one of the input terminals is used as the input, while both input terminals are used in the two-tone test. In the single-tone test, we applied an RF signal to the gate of the carbon nanotube transistor with frequencies of 1, 4, 8, 12, and 16 GHz sequentially, and varied its power level. A spectrum analyzer was used to measure the output signal power level. Figure 4(b) plots the output power vs. input power curves at different frequencies for the single-tone test. Based on the results of the single-tone test, P_{1dB} can be extracted to be between 8 to 14 dBm. Details of the extraction process can be found in the ESM (Fig. S2). Furthermore, we carried out the two-tone test for the ultra-high purity semiconducting carbon nanotube transistors. In the two-tone test, two RF signals with frequencies of 8 and 8.3 GHz were applied to the two input terminals as shown in Fig. 4(a), and a spectrum analyzer was used to monitor the output signal. Figure 4(c) shows the results for the two-tone test in the frequency range of 8 GHz. From Fig. 4(c), we can observe that the fundamental term increases with the input signal power with a speed of 10 dB/dec, while the third-order term increases with the input signal power with a speed of 30 dB/dec. The input third-order intercept point IIP_3 is extracted to be 18.3 dBm with an output third-order intercept point OIP_3 of 2.2 dBm. In theory, IIP_3 is about 9.6 dB higher than P_{1dB}. The P_{1dB} for the transistor at a frequency of 8 GHz is 8 dBm (Fig. S2 in the ESM). Results for the two-tone test and the single-tone test match well with each other. According to the above results, the linearity behavior of the ultra-high purity semiconducting carbon nanotube transistors is comparable to 180 nm complementary metal oxide semiconductor (CMOS) transistors [33, 34].

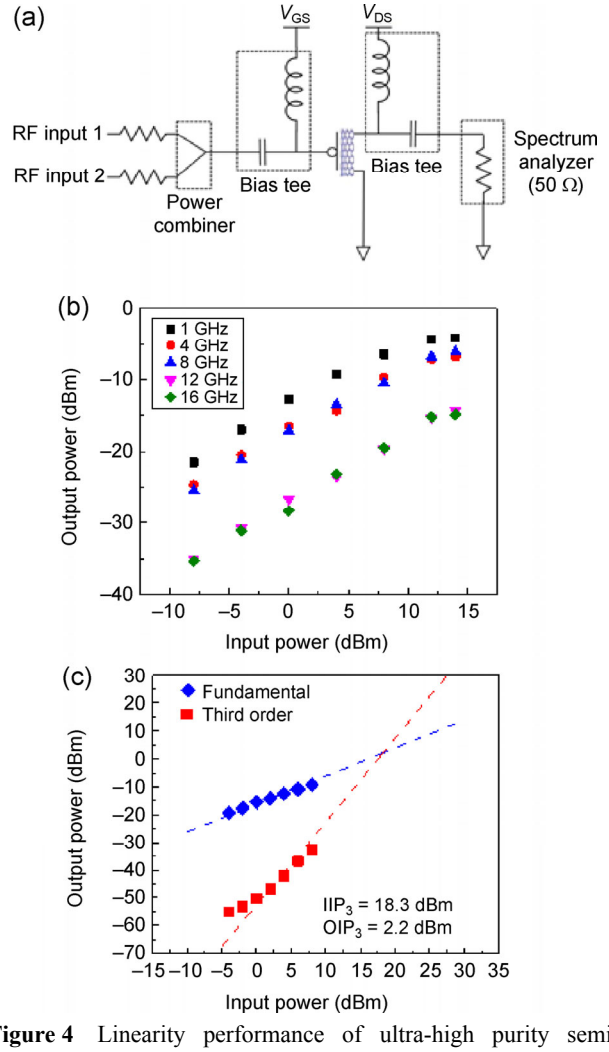

Figure 4 Linearity performance of ultra-high purity semiconducting carbon nanotube transistors. (a) Schematic of the measurement setup for single-tone and two-tone tests. (b) Output power vs. input power curves at different frequencies for the single-tone test. (c) Output power vs. input power of the fundamental term and the third-order term in the frequency range of 8 GHz.

The ultra-high purity semiconducting carbon nanotube transistors can be used as mixers due to their good RF performance and good linearity behavior [23]. The transistors can be configured as a mixer with the setup shown in Fig. 4(a). In order to test the performance of the mixer, local oscillation (LO) signal and RF signal are mixed at the two input terminals. Figure 5(a) shows the mixer performance of a carbon nanotube transistor biased at V_{gs} = –1.5 V and V_{ds} = –1.5 V. The LO signal was chosen with a frequency of 4.2 GHz and power of –3 dBm, while the RF signal was chosen with a frequency of 4 GHz and power of

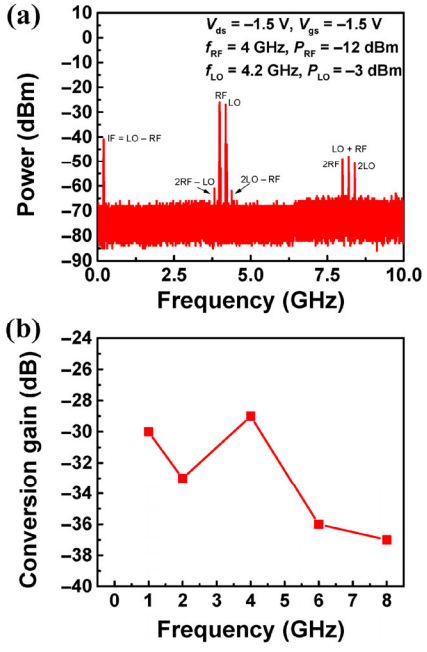

Figure 5 Mixer application of the ultra-high purity semiconducting carbon nanotube transistors. (a) Output spectrum of an ultra-high semiconducting carbon nanotube transistor configured as a mixer. (b) Conversion gain vs. frequency response of the same mixer.

–12 dBm. From the output spectrum of the mixer as shown in Fig. 5(a), one can find all the first-order (f_{RF}, f_{LO}), second-order ($2f_{RF}$, $2f_{LO}$, $f_{RF} + f_{LO}$, $f_{RF} - f_{LO}$), and third-order frequency ($2f_{RF} - f_{LO}$, $2f_{LO} - f_{RF}$) components of the mixer. The intermediate frequency ($f_{IF} = f_{LO} - f_{RF}$) for this mixer is 200 MHz with a power of –41 dBm. The conversion gain of this mixer is calculated to be –29 dB. We also tested the mixer at 1, 2, 6, and 8 GHz, and the results can be found in the ESM (Fig. S3). Figure 5(b) plots the conversion gain vs. frequency curve of the same mixer. The conversion gain decreases with the increase in the input RF signal frequency. Based on the above mixer test, the ultra-high purity semiconducting carbon nanotubes show a good potential for mixer applications.

3 Conclusions

In summary, we have made self-oxidized and self-aligned T-shape aluminum gate transistors with ultra-high purity semiconducting carbon nanotubes as the active channel material. The carbon nanotube transistors showed high transconductance and excellent current saturation behavior owing to their ultra-high purity. We carried out both DC and RF characterization for the carbon nanotube transistors. We achieved an extrinsic current gain cut-off frequency of 22 GHz and an intrinsic current gain cut-off frequency of 28 GHz. The extrinsic current gain cut-off frequency is the highest among all transistors based on carbon nanotube networks. Moreover, we achieved an extrinsic maximum oscillation frequency of 19 GHz and an intrinsic maximum oscillation frequency of 25 GHz. The extrinsic maximum oscillation frequency creates a record for all kinds of carbon nanotube transistors. Furthermore, we conducted single-tone and two-tone tests to characterize the linearity behavior of the ultra-high purity semiconducting carbon nanotube transistors. We achieved P_{1dB} between 8 to 14 dBm and an IIP_3 of 18.3 dBm. At last, we configured the ultra-high purity semiconducting carbon nanotube transistors as mixers, which work in the GHz frequency range. Our work sheds light upon the importance of ultra-high purity for the RF performance of carbon nanotube transistors and successfully improves the RF performance of carbon nanotube transistors to a new level. In addition, our work confirms the great potential for carbon nanotubes to be used as building blocks for RF circuits and systems.

4 Method

4.1 Ultra-high purity semiconducting carbon nanotube dispersion

Quartz substrates were used as the substrates to reduce parasitic capacitance. In order to get a uniform and high-density network, the ultra-high purity semiconducting carbon nanotube solution was first diluted by 10 times with xylene. Quartz substrates were then immersed into the diluted solution for 1 h and 15 min, followed by slightly rinsing with pure xylene solution. The quartz substrates were then put on a hotplate with a temperature of 200 ˚C for 1 h to remove the excessive solvents.

4.2 RF transistor fabrication process

First, titanium/palladium (1 nm layer thickness of Ti/50 nm layer thickness of Pd) were deposited by electron-beam as the source and drain electrodes.

Second, carbon nanotubes outside channel regions were etched away by oxygen plasma. The T-shape gate was patterned by electron-beam lithography and sequentially 140 nm layer thickness of aluminum was deposited by thermal evaporation and oxidized in air at 120 °C. Finally, 10 nm layer thickness of palladium was deposited by electron-beam as the self-aligned source and drain contacts, shortening the channel length to 120–140 nm.

Acknowledgements

We would like to acknowledge the collaboration of this research with King Abdul-Aziz City for Science and Technology (KACST) via The Center of Excellence for Green Nanotechnologies (CEGN). We also would like to acknowledge the Center for High Frequency Electronics (CHFE) at UCLA for technical support. We thank Dr. Han Wang at USC and Mr. Minji Zhu at CHFE for help with RF measurements, and we also thank Mr. Jefford J. Humes at NanoIntegris for helpful discussions.

Electronic Supplementary Material: Supplementary material (optical image of a typical self-aligned T-gate structure, open and short structure for de-embedding process, 1 dB gain compression point extraction process for the single tone test, and the mixer measurement results under various frequencies) is available in the online version of this article at http://dx.doi.org/10.1007/s12274-015-0915-7.

References

[1] Dürkop, T.; Getty, S. A.; Cobas, E.; Fuhrer, M. S. Extraordinary mobility in semiconducting carbon nanotubes. *Nano Lett.* **2004**, *4*, 35–39.

[2] Zhou, X. J.; Park, J. Y.; Huang, S. M.; Liu, J.; McEuen, P. L. Band structure, phonon scattering, and the performance limit of single-walled carbon nanotube transistors. *Phys. Rev. Lett.* **2005**, *95*, 146805.

[3] Rutherglen, C.; Jain, D.; Burke, P. Nanotube electronics for radiofrequency applications. *Nat. Nanotechnol.* **2009**, *4*, 811–819.

[4] Javey, A.; Wang, Q.; Ural, A.; Li, Y. M.; Dai, H. J. Carbon nanotube transistor arrays for multistage complementary logic and ring oscillators. *Nano Lett.* **2002**, *2*, 929–932.

[5] Derycke, V.; Martel, R.; Appenzeller, J.; Avouris, P. Carbon nanotube inter- and intramolecular logic gates. *Nano Lett.* **2001**, *1*, 453–456.

[6] Liu, X. L.; Lee, C.; Zhou, C. W.; Han, J. Carbon nanotube field-effect inverters. *Appl. Phys. Lett.* **2001**, *79*, 3329–3331.

[7] Ryu, K.; Badmaev, A.; Wang, C.; Lin, A.; Patil, N.; Gomez, L.; Kumar, A.; Mitra, S.; Wong, H. S. P.; Zhou, C. W. CMOS-analogous wafer-scale nanotube-on-insulator approach for submicrometer devices and integrated circuits using aligned nanotubes. *Nano Lett.* **2009**, *9*, 189–197.

[8] Shulaker, M. M.; Hills, G.; Patil, N.; Wei, H.; Chen, H. Y.; Wong, H. S. P.; Mitra, S. Carbon nanotube computer. *Nature* **2013**, *501*, 526–530.

[9] Cao, Q.; Kim, H. S.; Pimparkar, N.; Kulkarni, J. P.; Wang, C. J.; Shim, M.; Roy, K.; Alam, M. A.; Rogers, J. A. Medium-scale carbon nanotube thin-film integrated circuits on flexible plastic substrates. *Nature* **2008**, *454*, 495–500.

[10] Zhang, J. L; Fu, Y.; Wang, C.; Chen, P. C.; Liu, Z. W.; Wei, W.; Wu, C.; Thompson, M. E.; Zhou, C. W. Separated carbon nanotube macroelectronics for active matrix organic light-emitting diode displays. *Nano Lett.* **2011**, *11*, 4852–4858.

[11] Cao, X.; Chen, H. T.; Gu, X. F.; Liu, B.; Wang, W. L.; Cao, Y.; Wu, F. Q.; Zhou, C. W. Screen printing as a scalable and low-cost approach for rigid and flexible thin-film transistors using separated carbon nanotubes. *ACS Nano* **2014**, *8*, 12769–12776.

[12] Chen, H. T.; Cao, Y.; Zhang, J. L.; Zhou, C. W. Large-scale complementary macroelectronics using hybrid integration of carbon nanotubes and IGZO thin-film transistors. *Nat. Commun.* **2014**, *5*, 4097.

[13] Zhang, J. L.; Gui, H.; Liu, B. L.; Liu, J.; Zhou, C. W. Comparative study of gel-based separated arcdischarge, HiPCO, and CoMoCAT carbon nanotubes for macroelectronic applications. *Nano Res.* **2013**, *6*, 906–920.

[14] Takahashi, T.; Yu, Z. B.; Chen, K.; Kiriya, D.; Wang, C.; Takei, K.; Shiraki, H.; Chen, T.; Ma, B. W.; Javey, A. Carbon nanotube active-matrix backplanes for mechanically flexible visible light and X-ray imagers. *Nano Lett.* **2013**, *13*, 5425–5430.

[15] Wang, C.; Hwang, D.; Yu, Z. B.; Takei, K.; Park, J.; Chen, T.; Ma, B. W.; Javey, A. User-interactive electronic skin for instantaneous pressure visualization. *Nat. Mater.* **2013**, *12*, 899–904.

[16] Vuttipittayamongkol, P.; Wu, F. Q.; Chen, H. T.; Cao, X.; Liu, B. L.; Zhou, C. W. Threshold voltage tuning and printed complementary transistors and inverters based on thin films of carbon nanotubes and indium zinc oxide. *Nano Res.* **2015**, *8*, 1159–1168.

[17] Li, S. D.; Yu, Z.; Yen, S. F.; Tang, W. C.; Burke, P. J. Carbon nanotube transistor operation at 2.6 GHz. *Nano Lett.* **2004**, *4*, 753–756.

[18] Le Louarn, A.; Kapche, F.; Bethoux, J. M.; Happy, H.; Dambrine, G.; Derycke, V.; Chenevier, P.; Izard, N.; Goffman, M. F.; Bourgoin, J. P. Intrinsic current gain cutoff frequency of 30 GHz with carbon nanotube transistors. *Appl. Phys. Lett.* **2007**, *90*, 233108.

[19] Nougaret, L.; Happy, H.; Dambrine, G.; Derycke, V.; Bourgoin, J. P.; Green, A. A.; Hersam, M. C. 80 GHz field-effect transistors produced using high purity semiconducting single-walled carbon nanotubes. *Appl. Phys. Lett.* **2009**, *94*, 243505.

[20] Wang, C.; Badmaev, A.; Jooyaie, A.; Bao, M. Q.; Wang, K. L.; Galatsis, K.; Zhou, C. W. Radio frequency and linearity performance of transistors using high-purity semiconducting carbon nanotubes. *ACS Nano* **2011**, *5*, 4169–4176.

[21] Che, Y. C.; Badmaev, A.; Jooyaie, A.; Wu, T.; Zhang, J. L.; Wang, C.; Galatsis, K.; Enaya, H. A.; Zhou, C. W. Self-aligned T-gate high-purity semiconducting carbon nanotube RF transistors operated in quasi-ballistic transport and quantum capacitance regime. *ACS Nano* **2012**, *6*, 6936–6943.

[22] Ding, L.; Wang, Z. X.; Pei, T.; Zhang, Z. Y.; Wang, S.; Xu, H. L.; Peng, F.; Li, Y.; Peng, L. M. Self-aligned U-gate carbon nanotube field-effect transistor with extremely small parasitic capacitance and drain-induced barrier lowering. *ACS Nano* **2011**, *5*, 2512–2519.

[23] Che, Y. C.; Lin, Y. C.; Kim, P.; Zhou, C. W. T-gate aligned nanotube radio frequency transistors and circuits with superior performance. *ACS Nano* **2013**, *7*, 4343–4350.

[24] Steiner, M.; Engel, M.; Lin, Y. M.; Wu, Y. Q.; Jenkins, K.; Farmer, D. B.; Humes, J. J.; Yoder, N. L.; Seo, J. W. T.; Green, A. A. et al. High-frequency performance of scaled carbon nanotube array field-effect transistors. *Appl. Phys. Lett.* **2012**, *101*, 053123.

[25] Kocabas, C.; Dunham, S.; Cao, Q.; Cimino, K.; Ho, X. M.; Kim, H. S.; Dawson, D.; Payne, J.; Stuenkel, M.; Zhang, H. et al. High-frequency performance of submicrometer transistors that use aligned arrays of single-walled carbon nanotubes. *Nano Lett.* **2009**, *9*, 1937–1943.

[26] Wang, Z. X.; Liang, S. B.; Zhang, Z. Y.; Liu, H. G.; Zhong, H.; Ye, L. H.; Wang, S.; Zhou, W. W.; Liu, J.; Chen, Y. B. et al. Scalable fabrication of ambipolar transistors and radio-frequency circuits using aligned carbon nanotube arrays. *Adv. Mater.* **2014**, *26*, 645–652.

[27] Chaste, J.; Lechner, L.; Morfin, P.; Fève, G.; Kontos, T.; Berroir, J. M.; Glattli, D. C.; Happy, H.; Hakonen, P.; Placais, B. Single carbon nanotube transistor at GHz frequency. *Nano Lett.* **2008**, *8*, 525–528.

[28] Kocabas, C.; Hur, S. H.; Gaur, A.; Meitl, M. A.; Shim, M.; Rogers, J. A. Guided growth of large-scale, horizontally aligned arrays of single-walled carbon nanotubes and their use in thin-film transistors. *Small* **2005**, *1*, 1110–1116.

[29] Che, Y. C.; Wang, C.; Liu, J.; Liu, B. L.; Lin, X.; Parker, J.; Beasley, C.; Wong, H. S.; Zhou, C. W. Selective synthesis and device applications of semiconducting single-walled carbon nanotubes using isopropyl alcohol as feedstock. *ACS Nano* **2012**, *6*, 7454–7462.

[30] Li, J. H.; Liu, K. H.; Liang, S. B.; Zhou, W. W.; Pierce, M.; Wang, F.; Peng, L. M.; Liu, J. Growth of high-density-aligned and semiconducting-enriched single-walled carbon nanotubes: Decoupling the conflict between density and selectivity. *ACS Nano* **2014**, *8*, 554–562.

[31] Yeh, C. H.; Lain, Y. W.; Chiu, Y. C.; Liao, C. H.; Moyano, D. R.; Hsu, S. S. H.; Chiu, P. W. Gigahertz flexible graphene transistors for microwave integrated circuits. *ACS Nano* **2014**, *8*, 7663–7670.

[32] Badmaev, A.; Che, Y. C.; Li, Z.; Wang, C.; Zhou, C. W. Self-aligned fabrication of graphene RF transistors with T-shaped gate. *ACS Nano* **2012**, *6*, 3371–3376.

[33] Chen, J. D.; Lin, Z. M. 2.4 GHz high IIP3 and low-noise down-conversion mixer. In *Proceedings of the IEEE Asia Pacific Conference on Circuits and Systems*, Singapore, 2006, pp 37–40.

[34] Wan, Q. Z.; Wang, C. H.; Ma, M. L. A novel 2.4 GHz CMOS up-conversion current-mode mixer. *Radioengineering* **2009**, *18*, 532–536.